Solitary chemoreceptor cells in the nasal cavity serve as sentinels of respiration

Thomas E. Finger*†, Bärbel Böttger*, Anne Hansen*, Karl T. Anderson*, Hessamedin Alimohammadi‡, and Wayne L. Silver‡

*Department of Cellular and Structural Biology, Rocky Mountain Taste and Smell Center, Neuroscience Program, University of Colorado Health Sciences Center, Denver, CO 80262; and ‡Department of Biology, Wake Forest University, Winston-Salem, NC 27109

Edited by Theodore H. Bullock, University of California at San Diego, La Jolla, CA, and approved June 3, 2003 (received for review February 27, 2003)

Inhalation of irritating substances leads to activation of the trigeminal nerve, triggering protective reflexes that include apnea or sneezing. Receptors for trigeminal irritants are generally assumed to be located exclusively on free nerve endings within the nasal epithelium, requiring that trigeminal irritants diffuse through the junctional barrier at the epithelial surface to activate receptors. We find, in both rats and mice, an extensive population of chemosensory cells that reach the surface of the nasal epithelium and form synaptic contacts with trigeminal afferent nerve fibers. These chemosensory cells express T2R "bitter-taste" receptors and α-gustducin, a G protein involved in chemosensory transduction. Functional studies indicate that bitter substances applied to the nasal epithelium activate the trigeminal nerve and evoke changes in respiratory rate. By extending to the surface of the nasal epithelium, these chemosensory cells serve to expand the repertoire of compounds that can activate trigeminal protective reflexes. The trigeminal chemoreceptor cells are likely to be remnants of the phylogenetically ancient population of solitary chemoreceptor cells found in the epithelium of all anamniote aquatic vertebrates.

Most sensory systems use specialized sensory cells that link stimuli in the outside world to the nervous system. For example, rods and cones respond to visual stimuli, hair cells transduce auditory stimuli, taste receptor cells mediate perception of salt, sweet, sour and bitter, while olfactory receptor neurons detect the variety of odorants that fill our environment. However, no such specialized sensory cells have been identified that underlie the sensations of irritation or tickle when noxious substances like ammonia or pepper are inhaled into the nose (1). These sensations are conveyed through the trigeminal nerve; it is commonly assumed that the sensory elements for this system are free nerve endings of the neurons of the trigeminal ganglion, which express numerous receptors such as those for capsaicin and menthol (2, 3). Previous studies have shown that peptide-containing [substance P/calcitonin gene-related peptide (CGRP)] fibers of the trigeminal nerve, presumably polymodal nociceptors, provide a dense innervation to much of the respiratory epithelium (4), and end freely just below the level of the apical tight junctional complex (1, 5). The apparent junctional barrier separating the sensory nerve fibers from potential stimuli in the nasal cavity has been dismissed as an obstacle to chemosensory transduction, because many trigeminal chemical stimuli are lipid soluble and should diffuse easily across the junctional complex to reach the sensory nerve fiber. The mechanism by which lipophobic trigeminal stimuli might reach the sensory nerve fibers is less clear but has been hypothesized to involve a paracellular pathway (1). The presence of specialized epithelial chemosensory cells would provide a transduction system for detection of lipophobic stimuli, but such cells have yet to be demonstrated in the nasal cavity of any mammal. We report here that, in addition to free nerve endings, an extensive population of trigeminal chemosensory cells exists within the nasal respiratory epithelium, providing an avenue whereby inhaled toxic dusts or aerosols can trigger respiratory reflexes.

Methods

Histology. Fourteen rats and eight mice, ages 2–12 months, were anesthetized with sodium pentobarbital (150 mg/kg) and perfused transcardially or immersion fixed with 4% paraformaldehyde (PFA) in 0.1 M phosphate buffer (pH 7.2). We also examined the nose of one postnatal day 2 (P2) and three transgenic mice (from ages P4 to adult) in which the gustducin promoter drives GFP expression (6). For the gustducin-GFP mice (courtesy of Robert Margolskee, Mt. Sinai School of Medicine, New York), the tissue was visualized directly on epifluorescent dissecting and compound microscopes. For immunocytochemistry, the hemisected head was washed, treated with 0.5% hydrogen peroxide, blocked, and incubated in 1:2,000 rabbit anti-α-gustducin [directed against a peptide fragment containing amino acids 93–113 of α-gustducin; Gαgust (I-20): sc-395 (Santa Cruz Biotechnology)] for 2 days and reacted with the avidin–biotin complex (ABC) peroxidase method. To obtain transverse sections for charting reacted cells, heads were decalcified and 20-μm serial sections were cut on a cryostat.

Single-Label Immunocytochemistry. Standard avidin–biotin–peroxidase complex immunocytochemical procedures were used for visualization of the primary antiserum: 1:2,000 dilution of anti-Gαgust. For immunofluorescence, cryostat sections (20 μm) were incubated overnight at 4°C in the primary antibody against Gαgust (1:2,000), and visualized with the fluorescent secondary antibodies. Images were taken on an Olympus Fluoview confocal microscope. All gustducin immunoreactivity was eliminated by preabsorption of the antibody (diluted 1:10) with the cognate peptide at 0.5 μg/ml.

Double-Label Immunocytochemistry. For double labeling, we used the following antibodies: rabbit anti-ubiquitin carboxyl-terminal transferase (PGP 9.5) (Biogenesis, Bournemouth, U.K.), rabbit anti-CGRP (Chemicon), rabbit phospholipase C β2 [PLC β2; affinity-purified antibody directed against a carboxyl-terminal peptide; sc-206 (Santa Cruz Biotechnology; ref. 18)] and mouse anti-acetylated tubulin (Sigma). Mouse anti-acetylated tubulin (1:1,000) and rabbit anti-Gαgust (1:500) were applied as a mixture overnight at 4°C and reacted the next day with a mixture of secondary antisera with different fluorochromes. Antibodies raised in the same species were applied sequentially. After reacting the anti-Gαgust (1:500) with Alexa 568 goat anti-rabbit, washing in PBS, and blocking again for 3 h in blocking solution (see protocol above), the tissue was incubated either in rabbit anti-PGP 9.5 (1:1,000) or rabbit anti-CGRP (1:500) at 4°C and reacted the next day in the Alexa Fluor 488 secondary goat anti-rabbit (1:400). Alternatively, sections were first incubated in

This paper was submitted directly (Track II) to the PNAS office.

Abbreviations: PLC, phospholipase C; CGRP, calcitonin gene-related peptide; PGP 9.5, ubiquitin carboxyl-terminal transferase; SCC, solitary chemosensory cell.

†To whom correspondence should be addressed at: Department of Cellular and Structural Biology, University of Colorado Health Sciences Center, Room 4544, 4200 East Ninth Avenue B-111, Denver, CO 80262. E-mail: tom.finger@uchsc.edu.

anti-PGP 9.5 or anti-CGRP, then reacted with cobalt-intensified diaminobenzidine to yield a blue-black reaction product. The sections were then incubated in anti-gustducin or with anti-PLC β2, which was reacted with 3-amino-9-ethylcarbazole (AEC) to produce a red reaction product.

***In Situ* Hybridization and Gustducin Immunocytochemistry.** Sense and antisense riboprobes for the following gene products [mT2R5, mT2R8, and mT2R19 (bitter-taste receptors) and mT1R1 and mT1R2 (umami- and sweet-taste receptors)] were synthesized from cDNA incorporating digoxigenin-labeled UTP and unlabeled UTP at a 2:3 ratio, then hydrolyzed to an ≈500-bp length. Cryostat sections were treated with proteinase K (10 μg/ml), and then after washing, with 0.3% H_2O_2 to quench endogenous peroxidase. The slides then were incubated at 42°C in prehybridization buffer (50% deionized formamide/0.75 M NaCl/25 mM EDTA/25 mM Pipes, pH 6.8/1× Denhardt's solution/0.2% SDS/250 μg/ml polyadenylic acid/250 μg/ml salmon sperm DNA) for 1–2 h. Hybridization buffer (same as prehybridization with the addition of 5% dextran sulfate and 40–200 ng/ml of digoxigenin-labeled probe) was applied and allowed to hybridize overnight at 58–60°C. Digoxigenin label was detected with peroxidase-labeled sheep anti-digoxigenin antibody (Roche) diluted 1:500. After three rinses, trichostatin A (TSA)-cyanine 3 (Perkin–Elmer) diluted 1:100 in amplification buffer (Perkin–Elmer) was applied and allowed to react for 5–20 min. The sections then were washed and prepared for gustducin immunocytochemistry as described above. For whole-mount *in situ* hybridization, the hemisected head was pretreated and hybridized similarly to the sections. Probe was visualized by using alkaline phosphatase-labeled antidigoxigenin (Roche) reacted with 4-nitroblue tetrazoleum (NBT) and 5-bromo-4-chloro-3-indolyl-phosphate (BCIP) under alkaline conditions resulting in a dark blue chromogen. No reactive cells were observed when sense-strand control probes were used in place of the antisense probes.

Electron Microscopy. Adult rats were fixed overnight in buffered 4% PFA. The tissue was removed, embedded in egg yolk, and placed in fresh fixative for 12 h. The cryoprotected tissue block (7) was washed in PBS, and sectioned on a cryostat at 50 μm. The free-floating sections were incubated for 15 min in 0.5% hydrogen peroxide. After blocking in 3% BSA, 1% horse serum and 0.1% fish gelatin for 1.5 h, the tissue was incubated in anti-Gαgust (1:1,000) for 3 days at 4°C. The sections were placed overnight in biotinylated donkey anti-rabbit secondary antibody and reacted the next day in 0.02% diaminobenzidine for 3 min. Sections were postfixed in 5% glutaraldehyde and exposed to 1% osmium tetroxide for 30 min. Semithin sections were cut from flat-embedded (Epon/Araldite) blocks. Selected 3-μm-thick sections were reembedded. Ultrathin sections (silver to gold) were collected on formvar-coated slot grids, stained with uranyl acetate and lead citrate, and examined on a Philips (Eindhoven, the Netherlands) CM 10 electron microscope.

Ethmoid Nerve Recordings and Respiratory Monitoring. In brief (8), rats were anesthetized with ethyl carbamate (urethane: 1.0 g/kg of body weight) and two tracheal cannulae were inserted; one that allowed the rat to breathe room air, and a second inserted rostrally into the nasopharynx to permit delivery of fluids to the nasal cavity. A thermistor placed at the end of the respiratory cannula and connected to a Grass Instruments (Quincy, MA) P18 amplifier sufficed to monitor respiration. The rat was placed in a head holder with the ethmoid nerve exposed for several millimeters within the orbit. Multiunit activity was recorded by placing a nerve bundle on a pair of Pt-Ir wire hook electrodes connected to a Grass Instruments P511 preamplifier. The amplified neural activity was monitored with a Grass Instruments AM8 audio monitor and digitized, along with the respiratory data by using a Biopac MP100 data acquisition system and ACQKNOWLEDGE software (Biopac Systems, Goleta, CA). The chemosensory component of the neural response was calculated for each animal by subtracting the mean neural response to saline from the mean neural response to the chemical stimulus.

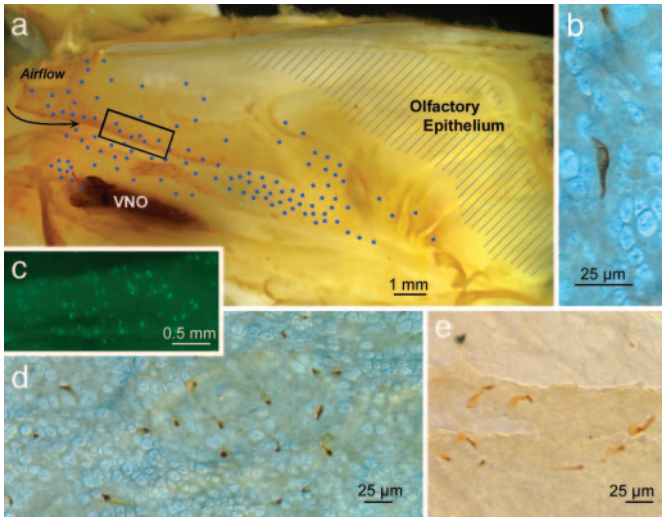

Fig. 1. Gustducin-expressing cells in the nasal epithelium. (*a*) The distribution of gustducin-immunoreactive cells on the turbinates and lateral nasal wall of a 6-week-old rat plotted on a lateral view of the nasal cavity split along the sagittal plane. The blue dots indicate the relative density and location of reactive cells. The region of olfactory epithelium is indicated by shading. The dark region at the left side of the figure is the vomeronasal organ (VNO). (Scale bar, 1.0 mm.) (*b*) Micrograph of an immunoreactive cell in the epithelium of a whole mount is shown. The elongate cell runs obliquely through the thin epithelium. (*c*) Fluorescent cells in the anterior portions of the nasal cavity, just caudal to the vestibule (boxed region in *a*), from an adult transgenic mouse in which GFP is driven by the gustducin promoter. The distribution of these fluorescent cells is similar to that revealed by gustducin immunocytochemistry. (*d*) Low-power micrograph of a field of gustducin-immunoreactive cells of a rat as revealed by whole-mount immunocytochemistry. The packing density of the scattered gustducin-containing cells varies according to the region of the nose in which they lie. In rats, the maximum density is ≈300 cells per mm^2. More often, the density is one order of magnitude less. Because of the convoluted nature of the nasal passageways and the variable density of gustducin-containing cells, it is difficult to give a reliable estimate of the total number of cells involved; however, in rat, the number on one side of the nose is >1,000. (*e*) Immunoreactive cells along the torn edge of the respiratory epithelium from a rat reacted as a whole mount. The apical portion of the cell is generally more immunoreactive (darker) than lower portions.

Results

The G protein α-gustducin is present in a variety of chemoreceptive cells, including some receptor cells in taste buds and chemosensory cells of the gut (9–11). When we examined the nasal epithelium with whole-mount immunocytochemistry for α-gustducin, we found widespread immunoreactive epithelial cells (Fig. 1) lining the medial (septum) and lateral walls of the anterior nasal cavity in both mice and rats. The immunoreactive cells are also present along the anteroventral edges of the anterior group of turbinates, i.e., facing the incoming airflow, and, as reported elsewhere (12, 13), in the anterior ducts of the vomeronasal organ. Another way to visualize the distribution of gustducin-containing cells is by use of a transgenic mouse, where the gustducin promoter drives expression of GFP (ref. 6; mice courtesy of Robert Margolskee). Fluorescent cells are prevalent in the rostral nasal cavity, just caudal to the vestibule as well as further ventrally in and around the anterior ducts of the vomeronasal organ. Thus, in mice as well as rats, gustducin-containing

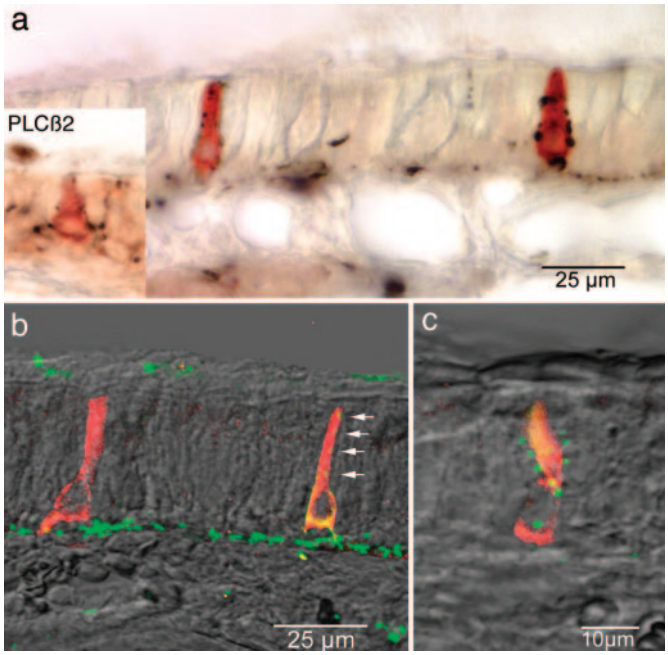

Fig. 2. Innervation of gustducin-immunoreactive epithelial cells as seen by double-label immunocytochemistry. In *a*, two elongate immunoreactive cells are apparent. Each is contacted repeatedly by PGP 9.5-immunoreactive nerve fibers (black). The gustducin-immunoreactive cells are not reactive for PGP 9.5, which reacts with other types of paraneurons. *Inset*, at the same magnification, shows a similar situation for a cell reacted with antisera to PLC β2, a downstream component in the T2R-gustducin transduction cascade. (*b* and *c*) Gustducin-immunoreactive cells (red-yellow) being contacted by CGRP-immunoreactive nerve fibers (green). Arrows in *b* indicate a series of neuronal varicosities in close proximity to the apical part of a gustducin-immunoreactive epithelial cell. The yellow color of the gustducin-immunoreactive cells is due to the double-labeling method employing primary antibodies raised in the same species. When CGRP antiserum is used without gustducin antiserum, the cells are not labeled (5).

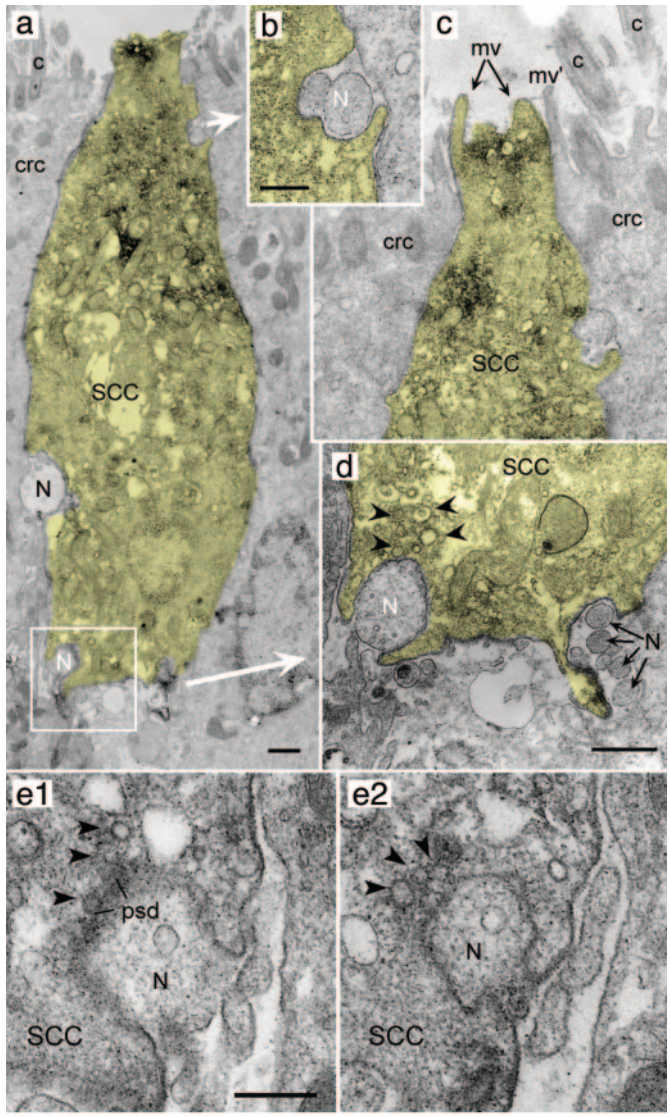

Fig. 3. Electron micrographs of a gustducin-immunoreactive epithelial cell. The dark flocculent reaction product marks the cytoplasm of the immunoreactive cell, which has been artificially tinted yellow for visibility. (*a*) The apical half of a gustducin-immunoreactive cell showing repeated contacts with nerve processes (N). (*b*) The contact between a nerve process and the apex of the cell. (*c*) From an adjacent section, the apex of the immunoreactive cell appears much narrower than the surrounding ciliated respiratory cells (crc). The microvilli (mv) of the immunoreactive cell are intermediate in size between the microvilli and cilia (c) of the ciliated respiratory cells. The microvilli of the gustducin-immunoreactive cell are wavy and have no subsurface filamentous web, unlike microvilli of respiratory brush cells. Scale as in *d*. (*d*, *e1*, and *e2*) Sites of specialized contact between the immunoreactive cells and nerve fibers display several features typical of synapses, including small vesicles (arrowheads) and a slight presynaptic thickening, are shown. The fine processes of a multiple branched nerve fiber (black N with arrows) are visible at the lower right in *d*. (*e1* and *e2*) Shown are nearby sections through a synaptic contact between an immunoreactive cell and a nerve fiber. Vesicles (arrowheads) are apparent within the chemoreceptor cell (SCC), whereas a modest postsynaptic density (psd) is visible in the nerve fiber. [Scale bars, 0.5 μm (*a* and *d*) and 0.25 μm (*b* and e).]

epithelial cells are scattered throughout the epithelium lining the airways of the anterior nasal cavity and ducts of the vomeronasal organ, i.e., regions devoid of olfactory or vomeronasal receptor cells.

The gustducin-immunoreactive epithelial cells vary in shape and size according to the type and thickness of epithelium they inhabit. Often the gustducin-immunoreactive cells are elongate and slant through the epithelium so that the immunoreactive cell is longer than the height of the epithelium. The cell bodies of the immunoreactive cells range in width from 5 to 10 μm; most taper to a narrow neck (2 μm or less) extending to the luminal surface (Fig. 2). At the surface of the epithelium, the gustducin-immunoreactive cells are significantly smaller than the surrounding, cylindrical cells (4–7 μm wide) of the respiratory epithelium (Fig. 3).

In order for a cell to serve as a chemoreceptor cell, it must exhibit an apical process, extending to the luminal surface, as well as a connection to the nervous system. Our ultrastructural studies reveal that the gustducin-immunoreactive cells possess a thin apical process with several microvilli extending into the nasal lumen. The microvilli are 90–100 nm in diameter and thus are quite different in appearance than the narrower (40–90 nm) microvilli of respiratory cells (Fig. 3*c*, mv) or the stiff, densely packed apical microvilli of respiratory brush cells (14).

To assess whether the gustducin-immunoreactive cells connect to the nervous system, we undertook dual-label immunocytochemistry by using markers found in trigeminal nerves innervating the nose: PGP 9.5, acetylated tubulin, and CGRP. In the vicinity of the gustducin-immunoreactive cells, the nerve fibers penetrate the basal lamina and turn toward the luminal surface in association with the gustducin-immunoreactive cells. The nerve fibers typically course along the length of the gustducin-immunoreactive cell, forming several varicosities along the way

toward the epithelial surface (Fig. 2*c*). Electron microscopic analysis of the gustducin-immunoreactive cells shows that the immunoreactive cells have numerous contacts with nerve fibers (Fig. 3). Often, the nerve fiber wraps around the gustducin-immunoreactive cell, sometimes enclosing it entirely (Fig. 3*b*). When the nerve fiber is embraced by the cell, the fiber may branch into 3–6 fine processes tapering down to 200–250 nm (Fig. 3*d*). Synaptic specializations are present (Fig. 3*e*) and look similar to the synaptic specializations found in taste buds (15). Synaptic vesicles (40–60 nm) within the gustducin-immunoreactive cells are translucent or contain dark cores (Fig. 3 *d* and *e*, arrowheads). Presynaptic and postsynaptic densities are present but are indistinct (Fig. 3*e*).

Many of the gustducin-expressing cells of taste buds and of the gut express mRNA coding for members of the T2R family of bitter-taste receptors (16, 17). To determine whether the gustducin-immunoreactive cells of the nose express T2R mRNA, we undertook *in situ* hybridization of both whole mounts and of sections through the nose in mice by using probes directed against three members of the T2R family of receptors. These findings reveal that the gustducin-immunoreactive nasal cells express mRNA for mT2R8 and mT2R19 (Fig. 4*a*). We did not, however, detect mT2R5 in this population of cells. In addition, the gustducin-immunoreactive cells also express PLC β2 (Fig. 2*a Inset*), a downstream component of the bitter-tastant transduction cascade in taste buds (18). *In situ* hybridization using probes to two other taste receptor molecules (T1R1 and T1R2) showed no hybridization with nasal chemosensory cells (see Fig. 5, which is published as supporting information on the PNAS web site, www.pnas.org) although a robust signal was present in palatal taste buds in the same tissue sections. The data indicate that the α-gustducin-expressing chemosensory cells of the anterior nasal cavity express much of the molecular machinery suitable for detection of bitter-tasting substances.

We next tested whether the trigeminal system responds to stimulation by bitter-tasting substances. Whole-nerve recordings from the ethmoid branch of the trigeminal nerve in rats demonstrate clear responses when the nasal epithelium is exposed to prototypical bitter substances, including denatonium [a charged, lipophobic substance and the normal ligand for mT2R8), quinine and cycloheximide (Fig. 4*b*)]. In contrast, the high-potency artificial sweetener, SC45647, elicited no neural response even at 200 μM (see Fig. 6, which is published as supporting information on the PNAS web site), a concentration sufficient to evoke strong taste responses. Thus, the trigeminal system possesses sensory cells that express T2R bitter-taste receptor mRNA, and respond to stimulation by bitter-tasting compounds. Detection of bitter-tasting compounds, often toxic substances, by the trigeminal nerve would likely be perceived as irritating rather than as a bitter sensation because the trigeminal and taste nerves connect to distinct sensory systems within the brain. Indeed, stimulation of the nasal epithelium with each of the bitter-tasting compounds tested, produces significant respiratory effects including slowing of the respiratory rate and apnea (Fig. 4 *c* and *d*). These responses are typical of those produced by classical trigeminal irritants (1). This response profile further supports the hypothesis that when applied to the nasal cavity, bitter-tasting substances are perceived as irritants and not as tastes.

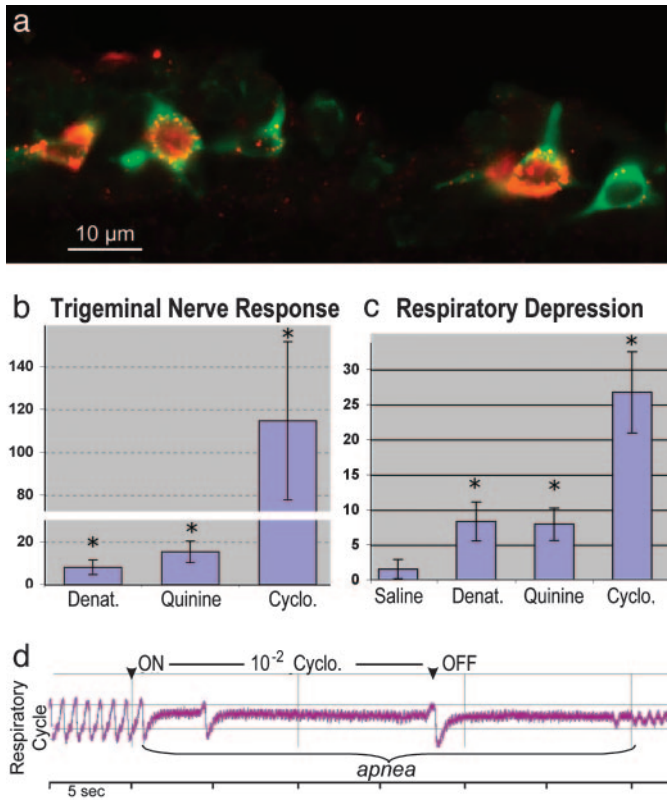

Fig. 4. Trigeminal chemoreceptors express T2R bitter-receptor mRNA and respond to stimulation with bitter-tasting ligands applied to the nasal passages. (*a*) Coexpression of mT2R8 (red, *in situ* hybridization) and gustducin (green, immunocytochemistry) in nasal SCCs. Although the gustducin immunoreactivity is evident throughout the cell, the *in situ* hybridization signal, which reveals the location of T2R8 mRNA, is perinuclear, where rough ER is typically located. (Scale bar, 10 μm.) (*b*) Relative chemosensory component (mean response to stimulus − mean response to saline) of the integrated neural activity in the ethmoid branch of the trigeminal nerve in anesthetized rats. The graph shows the percentage increase in neural activity during chemical stimulation compared with stimulation of the system with saline only. Responses to all compounds were significantly greater than responses to control (saline) solutions (*, paired *t* test, $P < 0.05$; six animals). Denat, denatonium (0.01 M); quinine (0.01 M); and Cyclo., cycloheximide (0.01 M). Error bars indicate SEM. (*c*) Mean percentage depression in respiratory rate when saline or bitter-tasting substances are applied to the nasal epithelium. The rate decreases significantly (*, paired *t* test, $P < 0.05$; nine animals) when the nasal epithelium is bathed in 0.01 M denatonium, quinine, or cycloheximide. Error bars indicate SEM. (*d*) Respiratory record in an anaesthetized rat is shown. The respiratory cycle is indicated by the sinusoidal purple line showing a basal respiration rate of approximately six breaths in 5 sec. A profound respiratory depression is evoked by 0.01 M cycloheximide. In this example, on application of cycloheximide, the steady prestimulus rate is drastically reduced to a near apnea (rate is less than one breath per 10 sec.). Shallow, but relatively normally paced respiration returns ≈10 sec after washout of the strong trigeminal stimulant.

Discussion

The nasal chemosensory cells we describe are situated at the anterior end of the nasal cavity behind the vestibule and along the anterior ducts of the vomeronasal organ. These sites are along the major path of airflow through the nasal cavity (19), and thus are ideally situated as sensory elements guarding against intake of potentially toxic substances. The sensory cells in the anterior nasal cavity monitor the incoming airstream, whereas the sensory cells in the vomeronasal ducts can guard against intake of toxic compounds in the fluids pumped through that organ (20).

The morphological features of the gustducin-immunoreactive cells in the nasal cavity of rodents are similar to those of solitary chemosensory cells (SCCs) described in epithelia of nonmammalian vertebrates (21). For example, the nasal epithelium of hagfish is replete with such cells (22), as is the olfactory epithelium of goldfish (23). The SCCs of nonmammalian vertebrates, like the gustducin-immunoreactive cells of the nasal cavity in rodents, form intimate, embracing contacts with branched nerve processes (21), many of which can arise from the

trigeminal nerve (22). Despite the phylogenetically wide abundance of SCCs throughout the nonmammalian vertebrates, such cells are not generally described for mammals. Three previous reports (12, 13, 24) describe the presence of potential SCCs in mammals, but their degree of similarity to the SCCs of aquatic anamniote vertebrates is unclear. Further, the SCC-like cells reported in mammals were limited to certain developmental stages or to restricted areas of specialized epithelia (13, 24). Likewise, the presence of T2R-expressing cells in the nasal cavity was noted (11), but the nature of such cells was not described. The use of taste receptor molecules by SCCs is not unique to rodents because SCCs and taste receptor cells in catfish apparently use a common taste receptor for arginine (25). Our results suggest that SCCs, known previously only in nonmammalian, aquatic vertebrates, are abundant within the nasal epithelium of rodents. Thus, this sensory system appears evolutionarily conserved in mammals, in contrast to the previously held belief that the system disappeared at the aquatic-terrestrial transformation in the vertebrate lineage.

The nasal SCCs in rodents are innervated by CGRP-immunoreactive fibers, presumably arising from the trigeminal nerve. Our previous experiments have shown that the CGRP-immunoreactive fibers of the nasal epithelium fall into the class of capsaicin-sensitive polymodal nociceptors (26), and usually also contain substance P. This histochemical profile is not consonant with nerve fibers of the other neural systems innervating the nasal cavity including the nervus terminalis [luteinizing hormone-releasing hormone (LHRH)-immunoreactive], olfactory, or vomeronasal nerves.

The nasal SCCs in rodents share several features with chemosensory cells elsewhere in the body. Dispersed oxygen-sensing pulmonary neuroendocrine cells are present throughout the respiratory tree (14, 27), but differ in several respects from the cells we describe in the nose. First, the pulmonary neuroendocrine cells, like other neuroendocrine cells, contain large apical secretory vesicles and exhibit immunoreactivity for PGP 9.5, neuron-specific enolase and peptides, including CGRP, whereas the SCCs of the nose do not. Second, the pulmonary neuroendocrine cells have a broad apex with a dense tuft of microvilli forming a brush border. The SCCs of the nose have a slender apex bearing only a few microvilli. Finally, the pulmonary neuroendocrine cells are innervated by the vagus nerve or peripheral autonomic nerves, whereas the nasal SCCs are innervated by the trigeminal nerve. Thus, the nasal SCCs are not identical to oxygen-sensing pulmonary neuroendocrine cells. The SCCs are like the pulmonary neuroendocrine cells in having repeated contacts with nerve fibers and numerous mitochondria. However, these are features common to many sensory cells, including taste cells and hair cells. Fujita (28) suggests that, based on morphological characteristics alone, brush cells of the airways might be chemosensory cells. The gustducin-immunoreactive cells we describe are not morphologically identical to brush cells as defined by Luciano *et al.* (14). A key characteristic of brush cells is the presence of numerous stiff apical microvilli with filamentous roots extending downward into the apical portion of the cell. Although the gustducin-ir cells have apical microvilli, the microvilli are not rigidly aligned as in brush cells and no filamentous roots are evident. Thus, the nasal gustducin-ir cells are not brush cells. Nonetheless, the gustducin-ir cells we find do fall into the class of paraneurons defined by Fujita (28), and which include taste bud cells and olfactory receptor neurons as well as enteroendocrine cells and brush cells. The nasal gustducin-expressing SCCs share features with some taste-receptor cells and with gut enteroendocrine cells. All of these chemosensory cell types express T2R receptors and gustducin, and respond to bitter-tasting substances (13, 17), but are quite different from one another in terms of morphology and relationship to local tissue elements. Thus, T2R receptor molecules should not be considered solely to be taste receptors, but rather chemoreceptors used by several chemosensory modalities.

Our results indicate the presence of an extensive array of chemosensory receptor cells scattered throughout the nasal epithelium of rodents. The cells express T2R (bitter taste) receptor mRNA and a G protein associated with other chemosensory cells; they possess an apical specialization similar to that of other chemosensory cells, and form synaptic contacts with peptidergic (CGRP-immunoreactive) nerve fibers of trigeminal origin, but are not associated with the olfactory, vomeronasal, or terminal nerves. The gustducin-immunoreactive cells are situated appropriately to monitor the incoming air stream for the presence of potential toxins; substances capable of evoking activity in the trigeminal nerve and eliciting reflexes such as apnea, coughing, or sneezing. The nasal chemosensory cells provide an avenue by which the trigeminal system can detect diverse compounds, including those unable to penetrate the epithelium to reach free nerve endings. Taken together, these results demonstrate the presence of a hitherto unknown receptor-cell population of the nasal cavity mediating vital protective reflexes, and thereby serving as sentinels for the airways.

We thank Robert Margolskee for allowing us to examine the gustducin-GFP transgenic animals; Charles Zuker (University of California at San Diego) and Nick Ryba (National Institutes of Health) for providing mT1R and mT2R probes; Nick Ryba and Mark Hoon for sharing unpublished data from their laboratory with us; Ms. Dot Dill for assistance in the preparation of some of the tissues for electron microscopy; and Drs. Linda Barlow, Angeles Ribera, Sue Kinnamon, and Nick Ryba for comments on various versions of this manuscript. This work was supported by National Institutes of Health Grants PO1 DC00244 and RO1 DC006070 (to T.E.F.).

1. Bryant, B. P. & Silver, W. L. (2000) in *The Neurobiology of Taste and Smell*, eds. Finger, T. E., Silver, W. L. & Restrepo, D. (Wiley, New York), pp. 73–100.
2. Liu, L. & Simon, S. A. (2000) *Physiol. Behav.* **69,** 363–378.
3. McKemy, D. D., Neuhausser, W. M. & Julius, D. (2002) *Nature* **416,** 52–58.
4. Silverman, J. D. & Kruger, L. (1989) *J. Comp. Neurol.* **280,** 303–330.
5. Finger, T. E., St. Jeor, V. L., Kinnamon, J. C. & Silver, W. L. (1990) *J. Comp. Neurol.* **294,** 293–305.
6. Huang, L., Shanker, Y. G., Dubauskaite, J., Zheng, J. Z., Yan, W., Rosenzweig, S., Spielman, A. I., Max, M. & Margolskee, R. F. (1999) *Nat. Neurosci.* **2,** 1055–1062.
7. Eldred, W. D., Zucker, C., Karten, H. J. & Yazulla, S. (1983) *J. Histochem. Cytochem.* **31,** 285–292.
8. Silver, W. L., Walker, D. B., Ogden, M. W. & Walker, J. C. (1990) *Chem. Senses* **15,** 701–712.
9. McLaughlin, S. K., McKinnon, P. J. & Margolskee, R. F. (1992) *Nature* **357,** 563–569.
10. Hofer, D., Puschel, B. & Drenckhahn, D. (1996) *Proc. Natl. Acad. Sci. USA* **93,** 6631–6634.
11. Adler, E., Hoon, M. A., Mueller, K. L., Chandrashekar, J., Ryba, N. J. & Zuker, C. S. (2000) *Cell* **100,** 693–702.
12. Sbarbati, A., Crescimanno, C., Benati, D. & Osculati, F. (1998) *J. Neurocytol.* **27,** 631–635.
13. Zancanaro, C., Caretta, C. M., Merigo, F., Cavaggioni, A. & Osculati, F. (1999) *Eur. J. Neurosci.* **11,** 4473–4475.
14. Luciano, L., Reale, E. & Ruska, H. (1968) *Z. Zellforsch. Mikrosk. Anat.* **85,** 350–375.
15. Kinnamon, J. C., Taylor, B. J., Delay, R. J. & Roper, S. D. (1985) *J. Comp. Neurol.* **235,** 48–60.
16. Chandrashekar, J., Mueller, K. L., Hoon, M. A., Adler, E., Feng, L., Guo, W., Zuker, C. S. & Ryba, N. J. (2000) *Cell* **100,** 703–711.
17. Wu, S. V., Rozengurt, N., Yang, M., Young, S. H., Sinnett-Smith, J. & Rozengurt, E. (2002) *Proc. Natl. Acad. Sci. USA* **99,** 2392–2397.
18. Clapp, T. R., Stone, L. M., Margolskee, R. F. & Kinnamon, S. C. (2001) *BMC Neurosci.* **2,** 6.
19. Kimbell, J. S., Godo, M. N., Gross, E. A., Joyner, D. R., Richardson, R. B. & Morgan, K. T. (1997) *Toxicol. Appl. Pharmacol.* **145,** 388–398.

20. Meredith, M. & O'Connell, R. J. (1979) *J. Physiol.* **286,** 301–316.
21. Whitear, M. (1992) in *Chemoreception in Fishes*, ed. Hara, T. J. (Elsevier, London), pp. 103–125.
22. Braun, C. B. (1998) *J. Comp. Neurol.* **392,** 135–163.
23. Hansen, A., Zippel, H. P., Sorensen, P. W. & Caprio, J. (1999) *Microsc. Res. Tech.* **45,** 325–338.
24. Sbarbati, A., Crescimanno, C., Bernardi, P. & Osculati, F. (1999) *Chem. Senses* **24,** 469–472.
25. Finger, T. E., Bryant, B. P., Kalinoski, D. L., Teeter, J. H., Bottger, B., Grosvenor, W., Cagan, R. H. & Brand, J. G. (1996) *J. Comp. Neurol.* **373,** 129–138.
26. Silver, W. L., Farley, L. G. & Finger, T. E. (1991) *Brain Res.* **561,** 212–216.
27. Van Lommel, A., Bolle, T., Fannes, W. & Lauweryns, J. M. (1999) *Arch. Histol. Cytol.* **62,** 1–16.
28. Fujita, T., Kanno, T. & Kobayashi, S. (1988) *The Paraneuron* (Springer, Tokyo).